Journal of the American College of Cardiology
© 2002 by the American College of Cardiology Foundation
Published by Elsevier Science Inc.

Vol. 39, No. 8, 2002
ISSN 0735-1097/02/$22.00
PII S0735-1097(02)01767-9

Near-Infrared Spectroscopic Characterization of Human Advanced Atherosclerotic Plaques

Jing Wang, PHD,* Yong-Jian Geng, MD, PHD,† Bujin Guo, PHD,* Tomas Klima, MD,* Birendra N. Lal, MD,† James T. Willerson, MD,*† Ward Casscells, MD*†

Houston, Texas

OBJECTIVES Living human carotid atherosclerotic plaques were examined in vitro by near-infrared (NIR) spectroscopy to determine the spectral features of plaque vulnerability.

BACKGROUND Plaque disruption, a major cause of heart attacks and strokes, cannot generally be predicted, but is thought to depend mainly on plaque composition. Near-infrared spectroscopy has been used to detect components in tissues noninvasively.

METHODS Using an NIR spectrometer fitted with a fiberoptic probe, living human carotid atherosclerotic plaques (from 25 patients) were examined ex vivo for plaque vulnerability. The plaques were cut into smaller sections according to their gross pathologic features, and NIR measurements were done at 20°C, usually within 10 min.

RESULTS According to the American Heart Association's recommended classification scheme, the lesions were classified into three groups: the first group comprised of vulnerable type V/VI lesions; the second group, stable type I/II lesions; and the third (intermediate) group, mainly type III/IV lesions. Cluster analysis of the specimens' NIR spectra identified three major composition groups in each of the three NIR spectral regions: 2,200 to 2,330 nm, 1,620 to 1,820 nm and 1,130 to 1,260 nm. Calculation of the lipid/protein ratios in each group at two NIR regions (2,200 to 2,330 nm) revealed ratios of 1.49 ± 1.20, 2.12 ± 1.00 and 3.37 ± 0.88 for type I/II, type III/IV and advanced type V/VI lesions, respectively ($p < 0.03$). At 1,620 to 1,820 nm, the respective ratios for these histologic groups were 0.57 ± 0.21, 1.54 ± 0.46 and 2.40 ± 0.44 ($p < 0.00003$).

CONCLUSIONS The good ex vivo discrimination of histologically vulnerable and stable plaques in this study suggests that NIR spectroscopy has the potential to identify vulnerable atherosclerotic plaques in vivo. (J Am Coll Cardiol 2002;39:1305–13) © 2002 by the American College of Cardiology Foundation

Atherosclerosis is recognized clinically as an arterial disease prominently involving the intima of medium- or large-sized arteries, including the aortic, carotid, coronary and cerebral arteries. Atherosclerotic lesions or plaques contain complex tissue matrix, including collagen, elastin, proteoglycans and extracellular and intracellular lipids with foamy macrophages and smooth muscle cells. In addition, inflammatory cellular components (e.g., T lymphocytes, macrophages, some basophils) also exist in the lesions. Disruption of atherosclerotic plaques appears to be the major cause of heart attacks and strokes. Although the risk of plaque rupture usually cannot be predicted, many postmortem examinations have revealed that this risk depends mainly on plaque composition (1,2). Most ruptured atherosclerotic plaques are characterized structurally by formation of a large, soft, lipid-rich, necrotic core covered by a thin fibrous cap densely infiltrated by macrophages. Inflammation is also a major feature of nonruptured, but eroded, thrombosed plaques.

Several clinical imaging techniques, such as ultrasonography, have been used, with limited success, in an effort to determine plaque stability (3–5). Although ultrasonic images provide anatomic information on plaque material and structure, it is difficult to determine plaque composition and to predict plaque vulnerability accurately and reliably from these images. High-resolution magnetic resonance imaging (MRI), a promising noninvasive technique for detecting plaque vulnerability (6,7), can distinguish the composition (e.g., large lipid pools, fibrous caps, calcifications) of atheromatous plaques, based on these components' physical properties (8).

Infrared (IR) spectroscopy is useful for identifying the chemical composition qualitatively and quantitatively. Molecular vibrational transitions measured in the near-infrared (NIR) region (750 to 2,500 nm) are multiquanta, single-photon, electric dipole transitions. Between 2,000 and 2,500 nm, NIR spectroscopy measures molecular stretching and bending combination motions. Above 2,000 nm, the NIR vibrational spectrum is dominated by overtone progressions, typically in X-H (X = C, N, O, etc.) stretching modes. The reduced photon absorption in the NIR region allows much deeper penetration, affording the possibility of in vivo

From the *Vascular Cell Biology Laboratory, Texas Heart Institute, and the †Division of Cardiology, Department of Internal Medicine, University of Texas Medical School at Houston, Houston, Texas. This study was supported by the U.S. Army's DREAMS Program (Disaster Relief and Emergency Medical Services) DoD grant no. DAMD 17-98-1-8002.

Manuscript received April 24, 2001; revised manuscript received January 23, 2002, accepted January 30, 2002.

Abbreviations and Acronyms
IR = infrared
MRI = magnetic resonance imaging
NIR = near-infrared

studies of human tissues. Combined with advanced data processing, chemometric analysis and fiberoptic technologies, NIR spectroscopy has been applied to biomedical fields and has demonstrated a substantial potential for diagnosing diverse clinical diseases (9,10).

Several groups (11,12) have used NIR and Raman spectroscopy to characterize and quantify the chemical composition of human atherosclerotic plaques in homogenized tissue sections and model systems. However, this technique has not been used to characterize living plaques. We hypothesized that metabolic and physiologic changes, together with changes in cell biology and chemistry of living atherosclerotic plaques, result in changes in the NIR spectral signature. These characteristic NIR spectral alterations may help identify vulnerable plaques with a thin cap and a large, lipid-rich, necrotic core. To examine this hypothesis as a step toward in vivo investigation, we evaluated the capability of NIR spectroscopy to determine the spectral features of plaque vulnerability in living human carotid atherosclerotic plaques in vitro.

METHODS

Human atherosclerotic plaque specimens. With the approval of the Institutional Review Boards of the Texas Heart Institute and St. Luke's Episcopal Hospital (Houston, Texas), human carotid atherosclerotic plaques removed from 25 patients by carotid endarterectomy were evaluated. The plaques were classified by gross pathologic examination and then cut into 145 smaller sections (each $\sim 6 \times 6$ mm^2), according to pathologic features.

Histologic analysis. After NIR measurement, the specimens were immediately analyzed histologically. Several locations representing the average of grossly observed changes were selected from each specimen and prepared for pathologic examination. The specimens were embedded in paraffin, cut into 4-μm-thick sections and deparaffinized, and the slides were stained with hematoxylin-eosin. The calcified areas of the specimens were decalcified using acid extraction. The plaque histologic classification was based on the American Heart Association's recommended classification scheme (13,14).

NIR spectroscopy and measurement techniques. To characterize the NIR absorption spectrum of the plaques' biochemical composition induced by cellular component changes, we used IR microspectroscopy to analyze freeze-dried, unstained, 25-μm-thin tissue sections from an area $\sim 10 \times 4$ mm^2 in the region of 1,700 to 2,500 nm. The section was placed onto a calcium fluoride window and allowed to dry. Using a spectrometer equipped with a $\times 15$ objective microscope (Bruker, Karlsruhe, Germany), we recorded 1,500 individual spectra (each covering 100×100 μm^2) at a resolution of 8 cm^{-1} for the selected tissue area. The NIR spectroscopic measurements were carried out in vitro at room temperature (20°C). The interval between plaque harvest and initiation of NIR measurements was usually $\leq$10 min. Under such conditions, these plaques were viable, as shown by their ability to proliferate in organ culture.

The NIR reflectance spectra of atherosclerotic plaques were measured using an NIR Systems model 6500 monochromator (Silver Spring, Maryland) with a fiberoptic-based SmartProbe sampling module. The system comprises a rugged NIR/VIS monochromator (75-W NIR light source) operated from a hand-held probe. The fiberoptic probe is a co-axial cable consisting of illumination (inner core: 210 fibers, 4.0 $\pm$ 0.5 mm diameter) and collection (outer core: 210 fibers, 6.5 $\pm$ 0.5 mm diameter) channels. The module's two detectors, PbS and Si, cover a spectral range of 400 to 2,500 nm, permitting use of visible and NIR wavelengths for sample characterization. For each measurement, 32 co-added scans were accumulated, and the ratio of that to a 32 co-added reference spectrum was calculated to obtain the absorption spectrum in log (1/reflectance) scale (collection time/spectrum, 35 s). Each specimen was measured three times, and the average of the three measurements taken as the final spectrum.

The penetration depths of the NIR signal to the aortic tissues were evaluated by placing a synthetic material—latex (Killian Latex, Inc., Akron, Ohio)—under the aortic tissue sections. Section thickness was measured in micrometers. The synthetic material has an NIR absorption signature that does not exist in human or animal tissue spectra. This absorbance signal band can act as a tracer to monitor attenuation of the absorption signal after the addition of each tissue layer, thus providing the NIR signal penetration depths of the aortic tissues. We estimated that at 75 W radiation power, the NIR signal penetrated into the aortic tissues to $\sim$350 μm, 750 μm and 1,000 μm in the spectral regions of 2,200 to 2,330 nm, 1,620 to 1,820 nm and 1,130 to 1,260 nm, respectively.

Treatment of data and statistics. Vision software (equipped with the NIR Systems) was used for data acquisition. Galactic spectral analysis software (Grams/32; Galactic Industries Corp., Salem, New Hampshire) was applied for data preprocessing. The ASCII data of second-derivative spectra were exported into Statistica, version 5.1 (StatSoft, Tulsa, Oklahoma) for classification.

Spectroscopic analysis of "living" tissue is more difficult because of strong water absorption bands that mask important absorption features arising from the specimen's biochemical constituents. Another problem is baseline fluctuation. To resolve these problems and to obtain detailed biochemical absorption features, we applied the second-derivative method—mathematical manipulation of spectra. The original NIR spectra were calculated using a 25-point

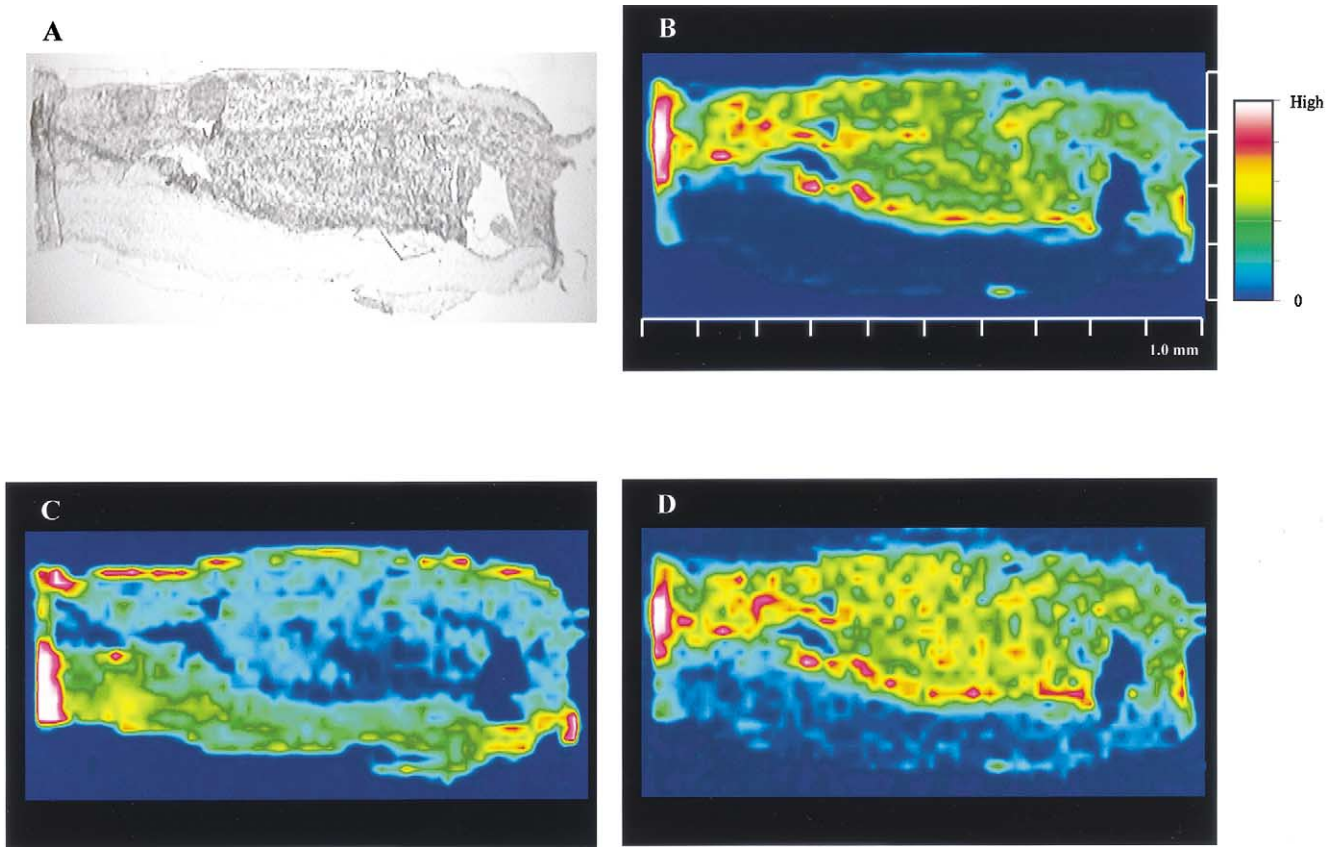

Figure 1. Spectroscopic images of a thin (25 μm), freeze-dried section of vulnerable human carotid atherosclerotic plaque in the near-infrared radiation region. **(A)** Regular light image of a plaque section. **(B to D)** Color near-infrared images illustrating the pattern of spectroscopic alteration. Major biochemical components are visualized by wavelength. **(B)** At 2,225 to 2,550 nm, the contents of cholesterol and cholesterol esters are shown from high to low in **red** to **orange** to **yellow** to **green** to **blue**. **(C)** At 2,200 to 2,225 nm, the contents of protein components (mainly collagen and other matrix proteins) are shown. **(D)** At 1,720 nm, lipid-rich regions **(red)** tend to co-localize with regions not in cholesterol (as in **B**).

Savitzk-Golay method (Grams/32) for the second derivative.

Statistical analysis. The NIR data were evaluated by cluster analysis, which uses the components of each spectrum to construct an informative classification of an initially unclassified data set. Three spectroscopic regions (2,200 to 2,330 nm, 1,620 to 1,820 nm and 1,130 to 1,260 nm) were selected for calculating the interspectral distance matrix and data classification. The distances between clusters were evaluated by Ward's method of analysis of variance. The geometric distances in the multidimensional space were measured.

RESULTS

Characterizations of canine aortic tissue and human atherosclerotic plaques by NIR spectroscopy. Using IR microspectroscopy to determine the major NIR spectroscopic features of advanced lesions (Fig. 1), we could visualize the major biochemical components by wavelength. The pseudo-color codes, ranging from blue to green to yellow to white, indicate variations (from low to high) in absorption intensities of lipid and protein components. Figure 2 shows the NIR spectra of the canine normal aorta with or without lipid deposits added. We found that spectra varied as lipid component amounts varied. The three spectral regions demonstrated changes when the amounts of lipid components varied. At 2,200 to 2,330 nm, with C-H stretching and bending combination motions normal, the aortic tissue did not appear to have an absorption signature at 2,304 nm, a feature that characterized the C-H combination derived from lipids (Fig. 3B). At 1,620 to 1,820 nm, with the C-H stretching first-overtone motions normal, the tissue had an absorbance band at 1,730 nm (Fig. 3C). As lipid component amounts increased, this absorption band shifted to 1,721 nm, with an enhanced intensity. The spectral pattern in this region also changed when the lipid components increased. At 1,130 to 1,260 nm, with C-H stretching second-overtone motions, the absorption intensities were lower than those in combination and first-overtone regions in normal tissue. Spectral changes, however, could be detected as lipid components increased. This was particularly apparent at the 1,204-nm region, where normal aortic tissue showed no absorption band. The composition of human atherosclerotic plaques is far more complex than that of canine normal aortic tissue with lipid deposits. Nevertheless, the NIR spectra of human atherosclerotic plaques share many common features with the NIR spectra of biofluids and tissue specimens from humans and

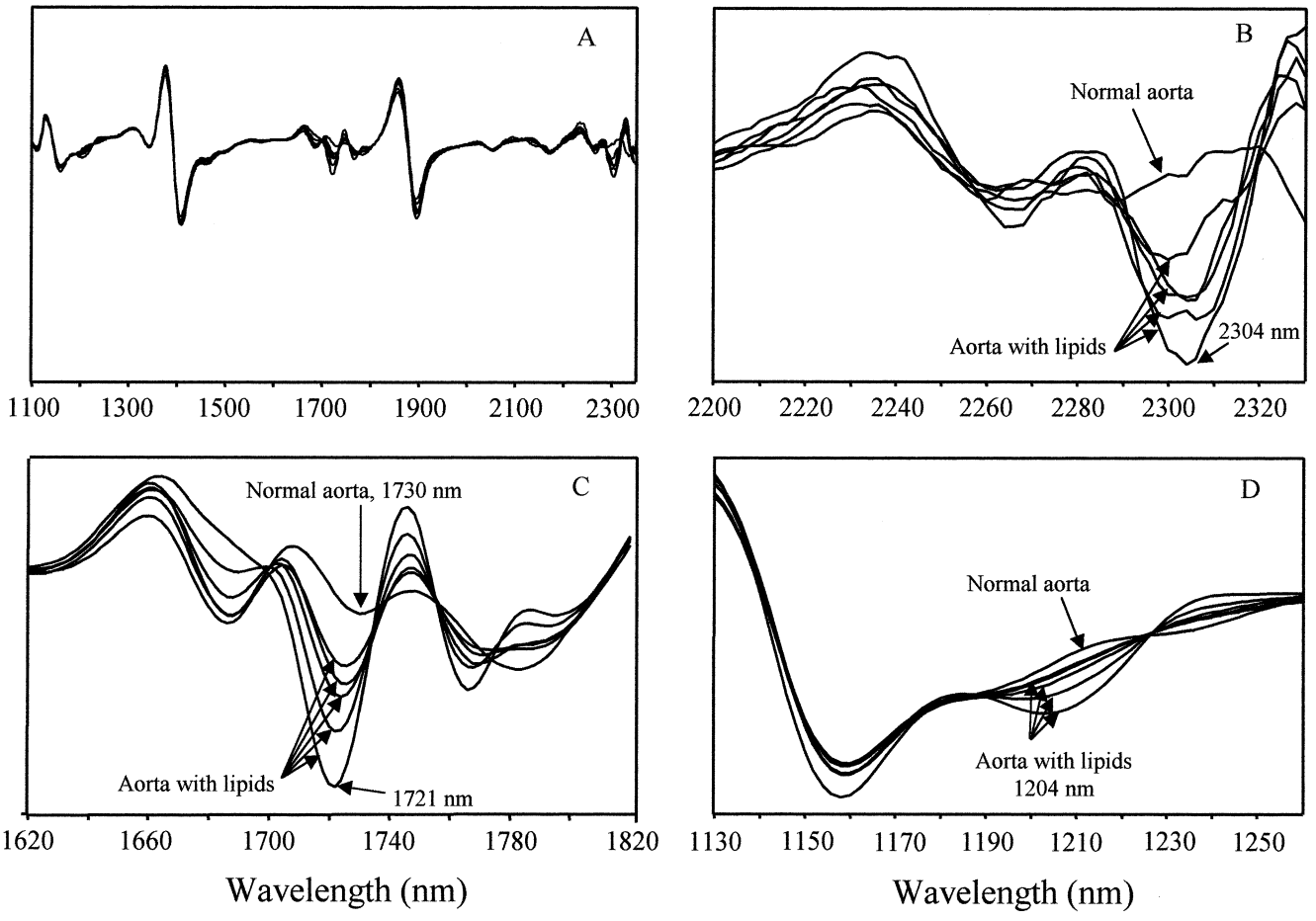

Figure 2. The near-infrared spectra of normal fresh (unfixed) canine aorta and canine normal aortic tissue overlaid with various amounts of lipid deposits (from carotid plaques in the same animal). **(A)** Overview of second-derivative near-infrared spectra in the region of 1,100 to 2,350 nm. Characteristic lipid shifts at 1,200, 1,720 and 2,300 nm were noted in all other animals, as well. Magnified views are shown in parts **B to D**. Spectra in the **(B)** long-range wavelength region (2,200 to 2,330 nm) and mid-range regions (**C**: 1,620 to 1,820 nm; **D**: 1,130–1,260 nm).

other animals. Typical NIR spectra of living human carotid atherosclerotic plaques in various histologic locations are shown in Figure 3. The lipid NIR signals were also detected by NIR spectrometry, clearly showing the shift and enhancement of absorbance bands at 1,130 to 1,204 nm.

Classification of NIR spectra. Hierarchical clustering statistical analysis of NIR spectra of living human carotid endarterectomy specimens identified three major composition groups in each of the three spectral regions (2,200 to 2,330 nm, 1,620 to 1,820 nm and 1,130 to 1,260 nm). As revealed by hematoxylin-eosin staining (Fig. 4), the first group displayed histologic features of type I/II lesions (stable fibrous plaques, mainly collagen layers with small amounts of inflammatory cells and limited lipids); the second group displayed features of vulnerable type V/VI lesions (advanced lesions containing soft, lipid-rich material, cholesterol crystals, inflammatory cells and fibrin); and the third (intermediate) group mainly displayed features of type II/IV lesions (fibroatheromatous material with calcium deposits, collagen mixed with thromboatheromatous material). The dendrograms of NIR spectral classification were observed in correlation with components in the three spectroscopic regions (Fig. 5).

We also calculated the lipid/protein ratio of each group at two NIR regions (2,200 to 2,330 nm and 1,620 to 1,820 nm) based on these regions' characterized absorption lipid and protein bands. At 2,200 to 2,330 nm, the lipid/protein ratios were 1.49 ± 1.20, 2.12 ± 1.00 and 3.37 ± 0.88 for type I/II, type III/IV and type V/VI lesions, respectively. One-way analysis of variance (Statistica) applied to the data set and post-hoc comparison using the Tukey multiple comparisons test demonstrated significant differences between the three groups ($p < 0.03$). At 1,620 to 1,820 nm, the respective lipid/protein ratios for the aforementioned histologic groups were 0.57 ± 0.21, 1.54 ± 0.46 and 2.40 ± 0.44. Statistical analysis, again, showed significant differences between these groups ($p < 0.0003$). Because of weak absorption features and highly overlapping phenomena at 1,130 to 1,260 nm, spectral specificity was lost. Associations between NIR classification, lipid/protein ratios and tissue histologic findings are presented in Table 1.

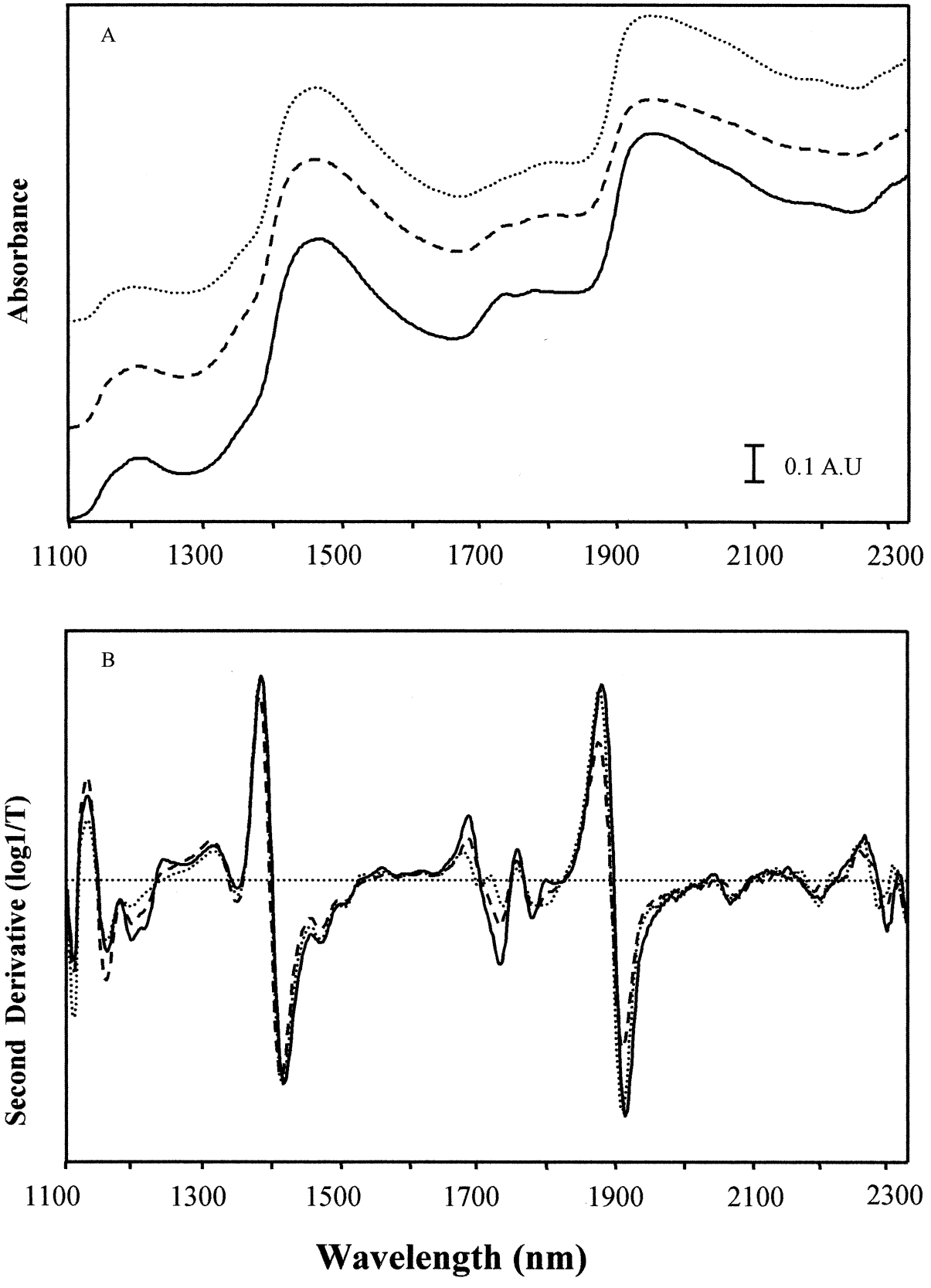

Figure 3. The near-infrared spectral features corresponding to the histologic features of human carotid atherosclerotic plaque. **(A)** The near-infrared spectra. The **dotted line** corresponds to the fibrous region; the **dashed line** to the calcified region; and the **solid line** to the yellow, soft region. The second derivative was also analyzed **(B)**, thereby reducing the heavy influence of the water signal. The three plaque regions became more homogeneous in signal, but some differences remained, particularly in the region of 1,660 to 1,750 nm. A.U. = absorbance units.

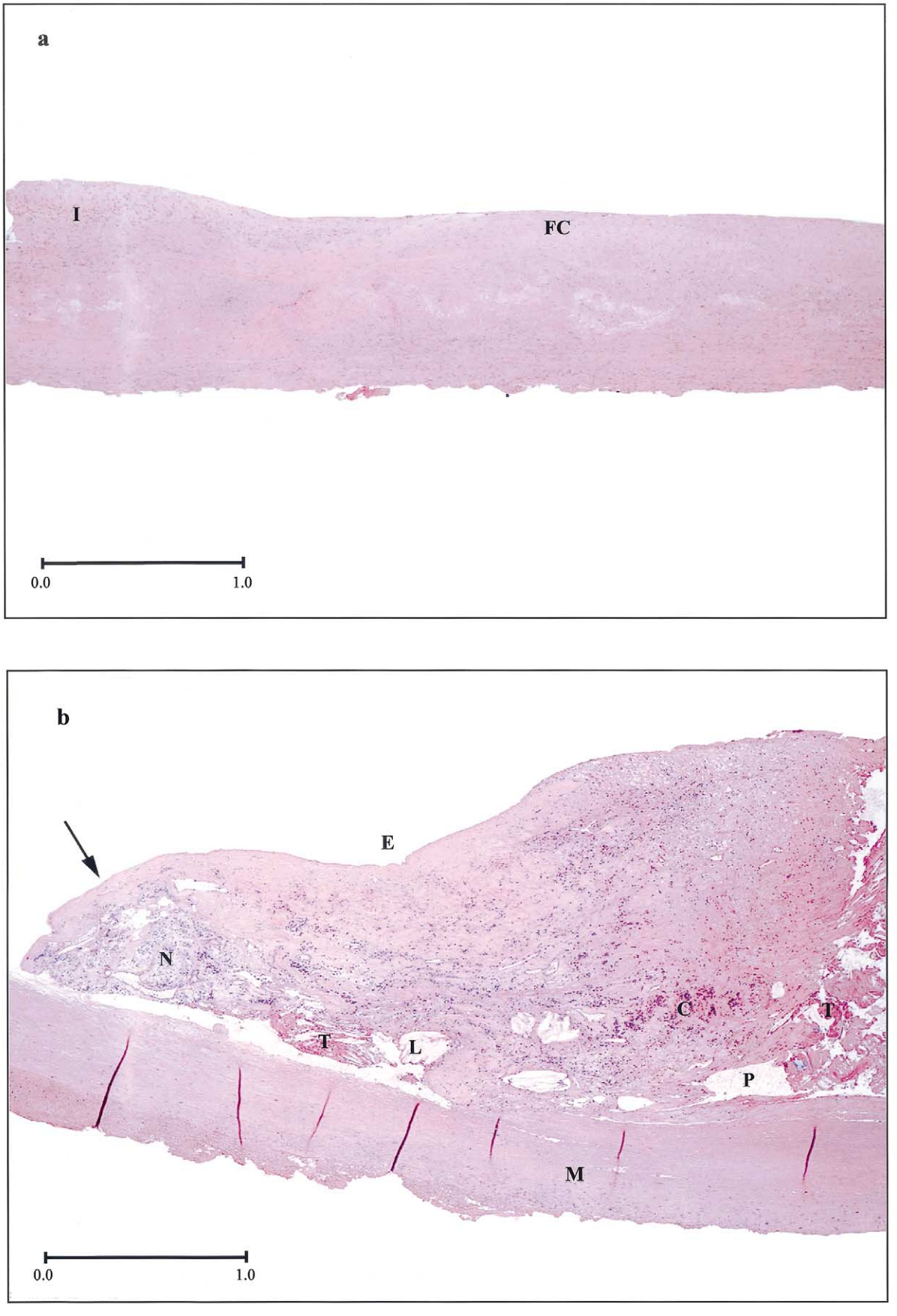

Figure 4. Photomicrographs illustrating the histopathologic findings of a portion of a stable, firm plaque, mostly collagen, with a few small areas of lipid deposits **(a)**, and an advanced atherosclerotic lesion in an unstable, soft plaque **(b)**. A thin cap **(arrow)** of ~150 μm is mainly composed of collagen layers. The necrotic core consists of lipids, cholesterol crystals (clefts), fibrin, lymphocytes and macrophages. Hematoxylin-eosin staining; magnification ×50. C = calcium; E = erosion; FC = fibrous cap; I = inflammation; L = lipid pool; M = medial layer; N = necrosis; P = platelet clump; T = thrombus.

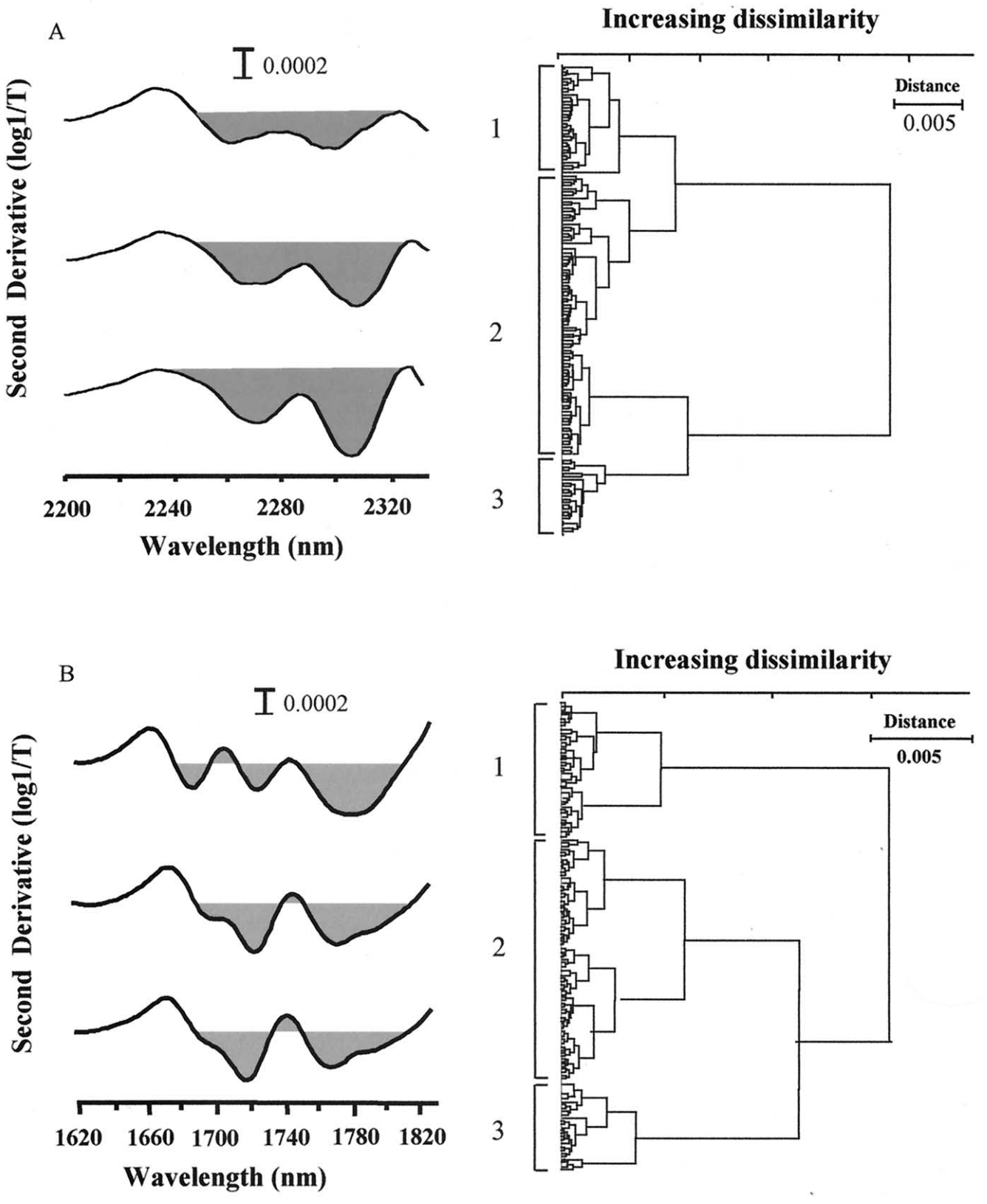

Figure 5. Cluster analysis yields an empiric classification of the NIR reflectance spectra of fresh atherosclerotic plaques from 25 patients. The plaques were divided into 145 fresh (living, unfixed) specimens and examined by near-infrared reflectance spectroscopy. Cluster analysis reveals three distinct groups **(right panels)** in each of two spectral regions: 2,240 to 2,320 nm **(A)** and 1,665 to 1,800 nm **(B)**. For each of the six cluster groups **(right panels)**, an average spectrum was calculated **(A and B)**. Group 1 specimens in the top and bottom panels correspond to American Heart Association (AHA) type I and II stable lesions. Group 2 specimens correspond to AHA type III and IV lesions. Group 3 specimens correspond to AHA type V and VI lesions.

Table 1. Near-Infrared Spectroscopic Determination of Lipid-to-Protein Ratio and Histologic Features of Atherosclerotic Plaques

Type of Lesions	NIR Wavelength Regions		Plaque Content		
	2,200–2,330 nm (Penetration Depth: ~350 μm)	1,620–1,820 nm (Penetration Depth: ~750 μm)	Lipids	Foam Cells	Inflammatory Cells
I/II	1.49 ± 1.20 (n = 34)	0.57 ± 0.21 (n = 42)	0%–5%	Low	Low
III/IV	2.12 ± 1.00 (n = 88)	1.54 ± 0.46 (n = 75)	5%–20%	Moderate	Mild
V/VI	3.37 ± 0.88 (n = 23)	2.40 ± 0.44 (n = 28)	20%–40%	High	Moderate

n = number of specimens; NIR = near-infrared.

DISCUSSION

Using IR microspectroscopy, we identified the major biochemical components within tissue sections, discriminated major types of atherosclerotic lesions and visualized site-to-site variability within living atherosclerotic lesions. The wavelengths characterizing the chemical components were shown to be useful in distinguishing the NIR spectra of living tissue and could have potential for developing in vivo NIR imaging techniques.

Potential clinical application. Compared with the NIR spectra of canine aortic tissue with added lipid deposits, the NIR spectra of human carotid atherosclerotic plaque specimens are far more complicated to analyze quantitatively, as they contain a greater variety of components. We observed that NIR spectroscopy combined with multivariate statistical analysis of atherosclerotic plaques demonstrates NIR features that correlate with morphologic and histopathologic findings, suggesting that the former combination has potential for clinical application.

However, when NIR spectra are collected and analyzed by histologic examination of the tissues, a problem can arise, mainly in sample preparation. In our study, histologic slides were prepared using only three or four thin sections across the sampled specimen (representing average tissue histology and cell biology), whereas the NIR spectra were collected over a much larger surface area to provide a spectroscopic description of particular depths (350, 750 and 1,000 μm) and a particular area (~33 mm^2). Thus, the histologic tissue sections did not fully reflect the morphologic and histopathologic findings of the investigated specimen. Moreover, although plaques were carefully cut (based on gross pathology of the tissues) into small portions for spectroscopic measurement, we could not completely avoid compositional overlapping. Thus, calcified tissue, for example, could contain other components, such as lipids. Larger study populations and smaller probes will likely improve the accuracy of classification.

As to why the spectrum of vulnerable plaques differs from that of less-inflamed, thicker-capped atheromas with a smaller necrotic core, we can only speculate that the higher lipid content of the vulnerable plaques accounts for some of the differences. In addition to structural differences, metabolic and physiologic variables, such as pH, triglycerides, glucose level and redox status, may also change the spectra in high-energy regions (15). The potential of NIR spectroscopy to determine these metabolic and physiologic variables and to correlate them with plaque vulnerability remains to be evaluated.

Challenges in identifying unstable plaques. With the clinical techniques (e.g., ultrasonography and MRI) currently available, identification of unstable plaques remains a challenge. The characteristics of vulnerable plaques include a large lipid-rich core, a thin fibrous cap, reduced collagen content and increased macrophage density and activity. The ability to detect the biochemical constituents (e.g., lipids, cholesterol, collagen) and cellular components (e.g., macrophages, lymphocytes) within the living plaques is essential for recognizing unstable plaques. Many studies revealed that lipid-rich cores with a high population of inflammatory cells characterize the majority of unstable plaques (16,17). The significant finding of our investigation is the characteristic NIR spectra of lipid-rich tissue with a thin fibrous cap. The ability of NIR spectroscopy to differentiate lipid-rich tissue from other plaque compositions suggests that this technique has the capability to distinguish unstable plaques.

The NIR pathologic investigation demonstrates that the cap is composed mainly of protein-rich, hypocellular fibrous connective tissue (Fig. 1B). Cap thickness is a crucial factor in plaque rupture. The relevant dimensions (25 to 200 μm) are difficult to resolve by intravascular ultrasonography and MRI. However, NIR radiation has a unique tissue penetration depth, which depends on the radiation wavelength, tissue properties and geometric design of the fiberoptic probe. Our investigations have shown that the average fiberoptic probe depth that allows collection of NIR radiation from the aortic specimen is ~1,000 μm in the region 1,130 to 1,260 nm, ~750 μm at 1,620 to 1,820 nm and ~350 μm at 2,200 to 2,330 nm. We hypothesize that the data derived from the 2,200 to 2,330-nm range may be the most relevant for predicting the behavior of plaques nearing the rupture stage. Such depths should be sufficient to penetrate into the thin cap and to carry some compositional information from various tissue depths.

Previous studies. Investigation by Casscells et al. (18) indicated that temperature heterogeneity in living atherosclerotic plaques may help identify plaques at risk of rupture and thrombosis. It has been determined that NIR spectra are sensitive to temperature variations (19); how such information on plaque stability will compare with IR thermography in the mid-IR radiation range (3 to 5 μm) is under investigation.

Charash et al. (20) reported that it is possible to detect

cholesterol in the rabbit aorta by means of a small (2.5 mm), specially designed fiberoptic catheter, combined with NIR reflectance spectroscopy. The spectral data in their investigation were obtained at 1,730, 1,745 and 1,760 nm. Our findings confirm the ability to identify vulnerable plaques in those regions. We describe an additional region (2,200 to 2,330 nm) where superficial plaque layers (~350 μm depth) can be detected, which may affect the prognostic ability. Finally, we developed a simple quantitative approach (protein/lipid ratio) to identify vulnerability in two NIR spectroscopic regions.

Study limitations. The major advantage of NIR spectroscopy is its potential for in vivo medical application, but this technique has some limitations. In general, NIR spectra have low absorptivity (reduced by about one-tenth as the vibration energy increases at each level) and large bandwidths that highly overlap. This characteristic strongly influences spectral analysis, particularly in differentiating the precise biochemical components (such as cholesterol and other lipid components) of a tissue section. Thus, we obtained "averaged" total protein and total lipid information from the NIR region.

Conclusions. Nevertheless, our findings indicate that changes in plaque composition, specifically those related to lipid-rich plaques that are unstable, will result in spectral changes. Although still in its infancy, the clinical application of NIR spectroscopy as a noninvasive tool is actively being explored. Our results suggest that NIR spectroscopy has the potential to identify vulnerable atherosclerotic plaques in vivo.

Acknowledgments

The authors thank Diane Hackett (Texas Heart Institute) for her editorial support, and B. Malik, MD (Texas Heart Institute) for his assistance during this study. We also extend special thanks to C. P. Schultz, PhD (Bruker Optics, Inc., Billerica, Massachusetts) for infrared spectroscopic imaging, and B. A. Deady and D. A. Deferrari (Cardiovascular Pathology Research, Texas Heart Institute, Houston, Texas) for microscopic images.

Reprint requests and correspondence: Dr. Ward Casscells, Division of Cardiology, Department of Internal Medicine, University of Texas Medical School at Houston, 6431 Fannin, P.O. Box 20708, Houston, Texas 77030. E-mail: S.Ward.Casscells@uth.tmc.edu.

REFERENCES

1. Willerson JT, Campbell WB, Winniford MD, et al. Conversion from chronic to acute coronary artery disease: speculation regarding mechanisms. Am J Cardiol 1984;54:1349–54.
2. Willerson JT, Golino P, Eidt J, et al. Specific platelet mediators and unstable coronary artery lesions. Circulation 1989;80:198–205.
3. Kleber FX, Döpfmer S, Thieme T. Invasive strategies to discriminate stable and unstable coronary plaques. Eur Heart J 1998;19 Suppl C:C44–9.
4. Bridal SL, Fornès P, Berger G. Relationship between ultrasonic attenuation, apparent integrated backscatter (30 to 50 MHz) and the composition of atherosclerotic plaque. In: Lees S, Ferrari L, editors. Acoustic Imaging. New York, NY: Plenum Press, 1997:181–6.
5. Wilhjelm JE, Gronholdt MLM, Sillesen H. Application of angle-dependence in the ultrasonic echo signal to estimation of carotic plaques contents. In: Lees S, Ferrari L, editors. Acoustic Imaging. New York, NY: Plenum Press, 1997:211–6.
6. Fayad ZA, Fallon JT, Shinnar M, et al. Noninvasive in vivo high-resolution magnetic resonance imaging of atheroslecrotic lesions in genetically engineered mice. Circulation 1998;15:1541–7.
7. Rader DJ. Noninvasive procedures for subclinical atherosclerosis risk assessment. Am J Med 1999;107:25S–7S.
8. Toussaint JF, LaMuraglia GM, Southern JF, et al. Magnetic resonance images lipid, fibrous, calcified, hemorrhagic, and thrombotic components of human atherosclerosis in vivo. Circulation 1996;94:932–8.
9. Kirkpatrick PJ, Lam J, Al-Rawi P, et al. Defining thresholds for critical ischemia by using near-infrared spectroscopy in the adult brain. J Neurosurg 1998;89:389–94.
10. Dempsey R, Davis DG, Buice RG, Lodder RA. Biological and medical applications of near-infrared spectrometry. Appl Spectroscopy 1996;50:18A–34A.
11. Römer TJ, Brennan JF, III, Fitzmaurice M, et al. Histopathology of human coronary atherosclerosis by quantifying its chemical composition with Raman spectroscopy. Circulation 1998;7:878–85.
12. Jaross W, Neumeister V, Lattke P, Schuh D. Determination of cholesterol in atherosclerotic plaques using near infrared diffuse reflection spectroscopy. Atherosclerosis 1999;147:327–37.
13. Virmani R, Kolodgie FD, Burke AP, et al. Lessons from coronary death: a comprehensive morphological classification scheme for atherosclerotic lesions. Arterioscler Thromb Vasc Biol 2000;20:1262–75.
14. Stary HC. Natural history and histological classification of atherosclerotic lesions: an update. Arterioscler Thromb Vasc Biol 2000;20:1177–8.
15. Guery BP, Mangalaboyi J, Menager J, et al. Redox status of cytochrome a,a_3: a noninvasive indicator of dysoxia in regional hypoxic or ischemic hypoxia. Crit Care Med 1999;27:576–82.
16. Kullo IJ, Willam D, Schwartz RS. Vulnerable plaque: pathology and clinical implications. Ann Intern Med 1998;129:1050–60.
17. Mann JDM. Vulnerable plaque: relation of characteristics to degree of stenosis in human coronary arteries. Circulation 1996;94:928–31.
18. Casscells W, Hathorn B, David M, et al. Thermal detection of cellular infiltrates in living atherosclerotic plaques: possible implications for plaque rupture and thrombosis. Lancet 1996;347:1447–9.
19. Barlow CH, Kelly KA, Kelly JJ. Tissue temperature by near-infrared spectroscopy. In: Chance B, Alfano RR, editors. Optical Tomography, Photon Migration and Spectroscopy of Tissue and Model Media. Bellingham, WA: International Society for Optical Engineering, 1995;2389:818–28.
20. Charash WE, Lodder RA, Moreno PR, et al. Detection of simulated vulnerable plaque using a novel near infrared spectroscopy catheter (abstr). J Am Coll Cardiol 2000;35 Suppl A:38.